J Huazhong Univ Sci Technol［Med Sci］
DOI 10.1007/s11596-012-1006-6 32(4):613-619,2012

Inhibitory Effects of Grape Seed Proanthocyanidin Extract on Selenite-induced Cataract Formation and Possible Mechanism

Xuan ZHANG (张 璇)[1, 2], Yizhen HU (胡义珍)[1#]
[1]*Department of Ophthalmology, Union Hospital, Tongji Medical College, Huazhong University of Science and Technology, Wuhan 430030, China*
[2]*Department of Ophthalmology, Children's Hospital of Chongqing Medical University, Chongqing 400014, China*

Summary: This study investigated the inhibitory effect of grape seed proanthocyanidin extract (GSPE) on selenite-induced cataract formation in rats and the possible mechanism. Eighty 8-day-old Sprague-Dawley rats were divided randomly into 5 groups: control group, model group, three GSPE groups (low dose, medium dose and high dose). Control group received subcutaneous injection of physiological saline. Model group was given subcutaneous injection of sodium selenite (20 μmol/kg body weight) on the postpartum day 10, and once every other day for consecutive three times thereafter. GSPE treated groups were respectively administered GSPE at doses of 50, 100, and 200 mg/kg body weight intragastrically 2 days prior to the selenite injection (that was, on the postpartum day 8), and once daily for fourteen consecutive days thereafter. The opacity of lenses was observed, graded and photographed under the slit lamp microscopy and the maximal diameter of the nuclear cataract plaques was measured. The lenses were analyzed for superoxide dismutase (SOD), catalase (CAT), glutathione peroxidase (GSH-PX), malondialdehyde (MDA), calcium (Ca^{2+}), nitric oxide (NO) and anti-hydroxyl radical ability (anti-OH^-). The histomorphology of lenses was observed with HE staining under a light microscope. The levels of calpainⅡ, and iNOS protein and mRNA expression in lenses were detected by using immunohistochemistry and real-time quantitative RT-PCR. The results showed subcutaneous injection of sodium selenite led to severe nuclear cataract in model group, and the achievement ratio of model group was 100%. As compared with model group, the degree of lenses opacity and the maximal diameter of nuclear cataract plaques were significantly reduced in GSPE-treated groups. Moreover, we observed selenite treatment caused a significant decrease in the activities of antioxidative enzymes (SOD, CAT, GSH-PX) and anti-OH^- ability, accompanied by a significant increase in the levels of MDA, NO, Ca^{2+} as well as iNOS, and calpainⅡ protein and mRNA expression. Administration of GSPE could dose-dependently preserve the activities of these antioxidative enzymes and anti-OH^- ability, accompanied by a significant reduction in the levels of MDA, NO, Ca^{2+} as well as iNOS, and calpainⅡ protein and mRNA expression. These results suggested that GSPE markedly prevented selenite-induced cataract formation probably by suppressing the generation of lipid peroxidation and free radicals as well as the activation of iNOS, and calpainⅡ in the lenses.
Key words: grape seed proanthocyanidin extract; selenite-induced cataract; oxidative stress; iNOS; calpainⅡ

Cataract accounts for 42% of blindness at present[1], affecting over 17 million of the nearly 45 million blind people worldwide with the highest incidence occurring in developing countries[2]. Although it can be remedied surgically by extirpation of the cataractous lens and substituting it with a lens made of synthetic polymers, various reasons such as increase in life span, postoperative complications, inhibition of undergoing surgery, poor doctor to patient ratio and so forth, the limitations in acceptability, accessibility, and affordability of cataract surgical services make it more relevant and important to look into alternative pharmacological measures for the treatment of this disorder[3].

Xuan ZHANG, E-mail: zx10170901@163.com
#Corresponding author, E-mail: 1012646376@qq.com

Although cataract is a multifactorial disease associated with several risk factors, oxidative stress has been suggested as a common underlying mechanism of cataract, and augmentation of the antioxidant defenses of the lens has been shown to prevent or delay experimental cataract[4].

There are several animal models of cataract nowadays, and selenite-induced cataract is an extremely rapid and convenient model of senile nuclear cataract with good repeatability[5]. The reliability and extensive characterization of selenite cataract has proved it to be the best rodent model for rapid screening of potential anti-cataract agents. The probable major mechanisms of selenite-induced cataract are loss of calcium homeostasis, reactive oxygen species generation, lipid peroxidation, calpain activation, insolubilization of proteins[6], etc.

Oligomeric proanthocyanidins, naturally existing

antioxidants widely available in fruits, vegetables, nuts, seeds, flowers and bark, have been reported to possess a broad spectrum of biological, pharmacological and therapeutic activities against free radicals and oxidative stress in both *in vitro* and *in vivo* models[7, 8]. The seeds of the grape are particularly rich source of proanthocyanidins, and has significantly superior scavenging ability to vitamin C, vitamin E and b-carotene[9].

It is reported that the activation of iNOS and calpain Ⅱ plays an important role in the process of cataract formation[10-12], but whether GSPE can suppress the activation of iNOS and calpain Ⅱ, and thus, prevent selenite-induced cataract formation has not been reported so far. In the present study, we assessed whether GSPE could retard selenite-induced cataract formation in the *in vivo* model and the possible mechanisms.

1 MATERIALS AND METHODS

1.1 Animals

Eighty 8-day-old Sprague-Dawley rats, weighing 15−20 g, were purchased from the Experimental Animal Center, Tongji Medical College, HUST, China. Rat pups were housed with their mother in an air-conditioned room at 23−25°C with a lighting schedule of 12 h light and 12 h dark. The animals were maintained on a standard laboratory animal diet and provided water *ad libitum* throughout the experimental period. The rat pups were divided randomly into five groups: control group, model group, and three GSPE groups (low dose, medium dose and high dose), 16 rat pups in each group (9 rat pups died and re-modeled again). Control group received subcutaneous injection of physiological saline. Model group was given subcutaneous injection of sodium selenite (20 μmol/kg body weight) on the postpartum day 10, and once every other day for continual three times thereafter[6]. GSPE (Tianjin Jianfeng Natural Product R&D Co, Ltd, China)-treated groups respectively were administrated GSPE at doses of 50, 100 and 200 mg/kg body weight intragastrically 2 days prior to the selenite (Heifei Bomei Biotechnology Company, China) injection (that was, on the postpartum day 8), and once daily for 14 consecutive days thereafter.

1.2 Morphological Examination of Cataract

The rat pups in each group were observed everyday from the day when their eyes opened (on the postpartum day 15). Before observation, the pupils were dilated with 1% atropine eye drops. The lens opacity was graded[13] (table 1) and photographed under the slit lamp microscopy on the postpartum day 21. The maximal diameter of the nuclear cataract plaques was measured using electronic vernier caliper from the postpartum day 15 to 21.

Table 1 Criterion of cataract grading by slit lamp in rats

Stages	Characteristic change in lens
0	Normal transparent lens
1	Initial sign of posterior subcapsular or nuclear opacity involving tiny scatters
2	Slight nuclear opacity with swollen fibers or posterior subcapsular scatterings
3	Diffuse nuclear opacity with cortical scatters
4	Partial nuclear opacity
5	Nuclear opacity not involving the lens cortex
6	Nature dense opacity involving the entire lens

1.3 Biochemical Analysis

Following the final administration of GSPE on the postpartum day 21, the rats were sacrificed by cervical dislocation, the bilateral eyes were immediately enucleated and the lenses were extirpated under a microscope, washed in ice-cold saline, weighed with electronic balance and stored at −80°C. The lenses were placed in vitreous homogenizer, and homogenized with physiological saline in 9 times their mass, then centrifuged at 3000 r/min for 10 min at 4°C. The supernatant obtained was used for the analysis of SOD, GSH-PX, CAT, MDA, anti-OH^-, Ca^{2+} and NO. All procedures were implemented according to the kit's instructions (Nanjing Jiancheng Bioengineering Institute, China), and analyzed by blind method.

1.4 HE Staining and Immunohistochemistry

The lenses were fixed in bouins solution for 6−8 h and then dehydrated through an ethanol series, embedded in paraffin. Four-μm consecutive sections were cut: a portion was submitted to conventional HE staining, and the rest reserved for immunohistochemistry. The expression of iNOS and calpain Ⅱ proteins was detected by using PV-9000 two-step immunohistochemical method (Beijing Zhongshan Goldenbridge Biotechnology Company, China). Paraffin-embedded sections were deparaffinized in xylene and hydrated with alcohol before being placed in 3% H_2O_2 methanol blocking solution in order to quench endogenous peroxidase, which was followed by heat-induced antigen retrieval. The slides were incubated with 1:200 dilution rabbit polyclonal antibodies against rat calpain Ⅱ or iNOS (Wuhan Boster Bioengineering Limited Company, China) overnight at 4°C, then stained using the PV-9000 detection system and counterstained with hematoxylin. All procedures were implemented according to the manufacturer's instructions. The positive cells of iNOS and calpain Ⅱ proteins were defined as that there were clearly yellow granules located in cytoplasm. The intensity of iNOS and calpain Ⅱ proteins was quantified using the image software (Imaging Pro Plus 6.0), and five visual fields were chosen randomly in every sample to calculate the average absorbance (*A*).

1.5 Real-time Quantitative RT-PCR

Total RNA was extracted from lenses using Trizol reagent (GIBCO, USA) according to the manufacturer's instructions. 2 μg of total RNA was reversely transcribed to first strand cDNA using M-MLV reverse transcriptase (Promega, USA). The real-time PCR was performed using SYBR Green Ⅰ fluorochrome (Biotium, USA), and standard curves of each group were obtained. The PCR conditions consisted of an initial denaturation at 94°C for 180 s, followed by amplification for 45 cycles of 30 s at

94°C, 30 s at 58°C and 30 s at 72°C. GAPDH was amplified as an internal control. Cycle threshold (Ct) values were measured and calculated by the CFX software. The amount of mRNA was normalized to GAPDH and calculated with the software Microsoft Excel. Relative mRNA content was calculated by a formula: $x=2^{-\Delta\Delta Ct}$, where $\Delta\Delta Ct=\Delta E-\Delta C$ and $\Delta E=Ct_{sample}-Ct_{GAPDH}$ and $\Delta C=Ct_{control}-Ct_{GAPDH}$[14]. Sequences of the primers used were shown in table 2 (Invitrogen, USA).

Table 2 Primer sequences used for real-time quantitative RT-PCR analysis

Primers		Sequence	Anneal temperature
iNOS	[s]	5′-CTTGGAGCGAGTTGTGGATTGT-3′	58°C
	[a]	5′-GTAGTGATGTCCAGGAAGTAGGT-3′	
Calpain Ⅱ	[s]	5′-CTGCGGATTCTGAGGCCGTTAC-3′	58°C
	[a]	5′-CTTCCCGGTCCACTCCACTTGT-3′	
GAPDH	[s]	5′-CACGGCAAGTTCAACGGCACAG-3′	58°C
	[a]	5′-ACGCCAGTAGACTCCACGACAT-3′	

1.6 Statistical Analysis

The analyses were carried out with SPSS 13.0 statistical software and the data expressed as $\bar{x}\pm s$. The data were statistically analyzed using analysis of variance (ANOVA), and *t* test was done in pairwise comparison. $P<0.05$ was considered to be statistically significant.

2 RESULTS

2.1 Morphological Assessment of Changes in Lens

At the final examination on the postpartum day 21, all rat pups were evaluated for cataract development and photographed (fig. 1). Control group developed clear lenses (stage 0), model group developed cataracts that were graded between stage 5 and 6 (fig, 1A and B), low dose GSPE group developed cataracts between stage 4 and 6 (fig. 1A−C), medium dose GSPE group developed cataracts between stage 2 and 5 (fig. 1B-E), and high dose GSPE group developed cataracts between stage 1 and 4 (fig. 1C−F).

Table 3 showed grading of the lens opacity of each group. As compared with model group, the degree of lenses opacity was significantly reduced in GSPE-treated groups ($P<0.05$ or $P<0.001$), and there were statistically significant differences between two GSPE-treated groups ($P<0.001$).

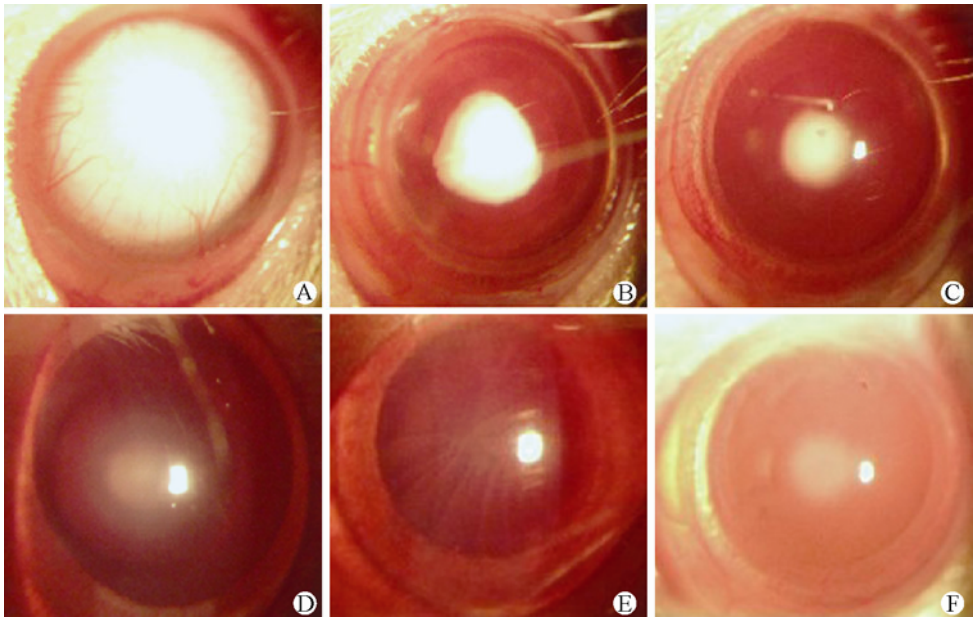

Fig. 1 Staging of selenite-induced cataract

A: Stage 6, mature dense opacity involving the entire lens; B: Stage 5, nuclear opacity not involving the lens cortex; C: Stage 4, partial nuclear opacity; D: Stage 3, diffuse nuclear opacity with cortical scatters; E: Stage 2, slight nuclear opacity with swollen fibers or posterior subcapsular scatterings; F: Stage 1, initial sign of posterior subcapsular or nuclear opacity involving tiny scatters

Table 4 showed the changes of maximal diameter of nuclear cataract plaques from the postpartum day 15 to 21. We observed that cataract had already been formed after three times of selenite injection in model group. The degree of the lens opacity and the diameter of nuclear cataract plaques were increased to varying degrees thereafter. In model group the degree of lenses opacity was the severest, the diameter of nuclear cataract plaques was the largest and its increasing was the fastest, whereas GSPE-treated groups manifested dose-dependent alleviation, the higher the dose the lighter the cataract. As compared with model group, the maximal diameter of nuclear cataract plaques had no statistically significant difference in low lose GSPE group from the postpartum day

15 to 18 (P>0.05), but significant reduction was found in medium dose and high dose GSPE groups (P<0.05 or P<0.01). Except that there were no statistically significant differences between medium dose and low dose GSPE groups from the postpartum day 15 to 16 as well as between medium dose and high dose GSPE groups from the postpartum day 15 to 18 (P>0.05), there were statistically significant differences between other adjacent two GSPE-treated groups (P<0.05 or P<0.01).

Table 3 Grading of the lens opacity

Groups	Stages							Number of lens	Mean stage
	0	1	2	3	4	5	6		
Model	−	−	−	−	−	15	17	32	5.53±0.51
GSPE									
Low dose	−	−	−	−	6	18	8	32	5.06±0.67*
Medium dose	−	−	3	12	15	2	−	32	3.50±0.76$^{**▲}$
High dose	−	5	12	8	7	−	−	32	2.53±1.02$^{**▲△}$

$^{*}P$<0.05, $^{**}P$<0.001 *vs.* model group; $^{▲}P$<0.001 *vs.* low dose GSPE group; $^{△}P$<0.001 *vs.* medium dose GSPE group

Table 4 Change in maximal diameter (mm) of nuclear cataract plaques

Groups	Diameter (mm)						
	Day 15	Day 16	Day 17	Day 18	Day 19	Day 20	Day 21
Model	1.58±0.24	1.66±0.13	1.76±0.25	1.85±0.03	1.93±0.18	2.00±0.28	2.10±0.25
GSPE							
Low dose	1.39±0.21	1.51±0.11	1.59±0.13	1.71±0.29	1.75±0.22*	1.79±0.20*	1.72±0.22**
Medium dose	1.13±0.36**	1.23±0.20**	1.29±0.08$^{**△△}$	1.30±0.23$^{**△△}$	1.34±0.19$^{**△△}$	1.40±0.26$^{**△△}$	1.44±0.12$^{**△△}$
High dose	0.92±0.27$^{**△}$	0.95±0.26$^{**△}$	1.00±0.04$^{**△△}$	1.04±0.10$^{**△△}$	1.07±0.17$^{**△△▼}$	1.08±0.06$^{**△△▼}$	1.19±0.10$^{**△△▼}$

$^{*}P$<0.05, $^{**}P$<0.01, *vs.* model group;$^{△}P$<0.05, $^{△△}P$<0.01 *vs.* low dose GSPE group; $^{▼}P$<0.05 *vs.* medium dose GSPE group

2.2 Biochemical Analysis

Table 5 showed the analysis of antioxidant enzymes (SOD, CAT, GSH-PX), MDA, NO, Ca^{2+} and anti-OH^{-} ability in lenses of rat pups. In low dose and medium dose GSPE groups, the activities of antioxidant enzymes (SOD, CAT, GSH-PX) and anti-OH^{-} ability were decreased, accompanied by a significant increase in the levels of MDA, NO, Ca^{2+} as compared with control group (P<0.01 or P<0.001), while there were no statistically significant differences between high dose GSPE group and control group (P>0.05). Administration of GSPE could dose-dependently preserve the activities of these antioxidative enzymes and anti-OH^{-} ability, and lead to a significant decrease in the levels of MDA, NO, and Ca^{2+} as compared with model group (P<0.05 or P<0.01 or P<0.001). There were statistically significant differences between adjacent two GSPE-treated groups (P<0.05 or P<0.01 or P<0.001).

Table 5 Biochemical indicators in lenses of selenite-induced cataract

Groups	SOD (U/mg protein)	GSH-PX activity	CAT (U/mg protein)	MDA (pm/ mg protein)	Anti-OH^{-} (U/mg protein)	NO (μmol/g protein)	Ca^{2+}(μmol/g protein)
Control	11.22±0.12	6.16±0.29	7.46±0.04	17.00±1.41	5.58±0.11	0.35±0.12	3.15±0.11
Model GSPE	3.27±0.31**	2.12±0.07*	3.70±0.18*	89.75±12.30**	2.01±0.15**	1.87±0.06**	20.00±2.03**
Low dose	4.86±0.11$^{**△}$	2.78±0.02$^{*△}$	4.01±0.21$^{*△}$	55.38±10.75$^{**△△}$	2.98±0.32$^{*△}$	1.25±0.13$^{☆△}$	12.52±1.65$^{**△△}$
Medium dose	7.09±0.45$^{*△▲}$	4.50±0.50$^{☆△▲}$	4.98±0.08$^{*△▲}$	31.75±2.50$^{*△△▼▼}$	3.80±0.43$^{☆△▲}$	0.88±0.09$^{☆△▲}$	9.10±1.02$^{**△△▲}$
High dose	9.08±1.09$^{▽▼#}$	5.28±0.51$^{▽▲#}$	6.56±0.17$^{△▲#}$	22.00±3.65$^{△△▼▼#}$	4.62±0.18$^{▽▲#}$	0.47±0.16$^{▽▲#}$	4.78±0.32$^{△△▼##}$

$^{☆}P$<0.05, $^{*}P$<0.01, $^{**}P$<0.001 *vs.* control group; $^{△}P$<0.05, $^{▽}P$<0.01, $^{△△}P$<0.001 *vs.* model group; $^{▲}P$<0.05, $^{▼}P$<0.01, $^{▼▼}P$<0.001, *vs.* low dose GSPE group; $^{#}P$<0.05, $^{##}P$<0.01 *vs.* medium dose GSPE group

2.3 HE Staining of Lens

As shown in fig. 2, HE staining of lens specimens showed the pink cytoplasm and blue nuclei. In control group the lens epithelial cells (LECs) were in linear arrangement, nuclei appeared elongated rod-shaped, with uniform morphology, the lens fiber layers were closely and regularly arranged, and the apex and base of the LECs were closely connected with the anterior lens capsule and lens fibers (fig. 2A). In model group, the lens fiber layers were disordered; more vesicles and water

split appeared between lens fiber layers; LECs proliferated, arranged irregularly with non-uniform cell gaps and swelled; pleomorphic nuclei, and a large number of lightly stained cytoplasm and vacuolization were seen (fig. 2B). In GSPE-treated groups the LECs had lighter damage than model group, and there was a dose-effect relationship, the higher the dose the less the damage. In low dose GSPE group, the LECs appeared in linear arrangement, the cells were irregular with pleomorphic nuclei, and more vesicles and water split appeared between fiber layers (fig. 2C). In medium dose GSPE group, LECs were in linear array with irregular shape and pleomorphic nuclei, the lens fiber layers were tightly packed, and LECs were closely collected with anterior capsule and lens fiber layers (fig. 2D). In high dose GSPE group, histomorphology of the LECs was similar to that in control group (fig. 2E).

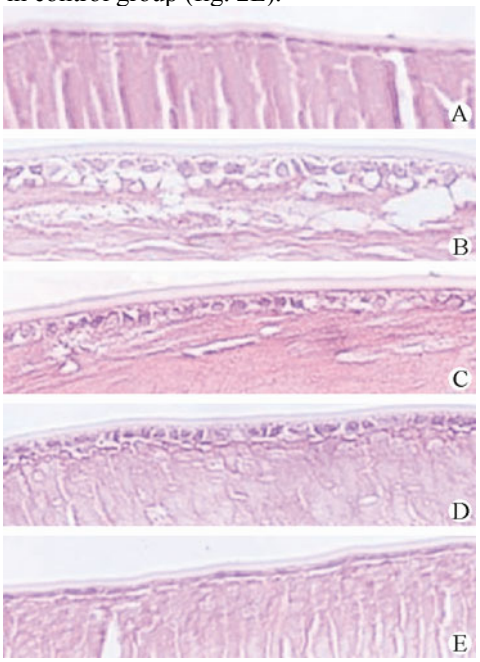

Fig. 2 Histomorphological observation of the lenses (HE,×40)
A: Control group; B: Model group; C: Low dose GSPE group; D: Medium dose GSPE group; E: high dose GSPE group

2.4 The Expression of INOS and Calpain Ⅱ Protein in Lenses

As shown in fig. 3 and 4, negative staining was found in control group which showed no positive granules in cytoplasm under a light microscope (fig. 3A and 4A). A large number of dark brown granules were found in cytoplasm of model group (fig. 3B and 4B). In GSPE-treated groups, the intensity of positive-staining LECs was weakened with the increasing dose of GSPE: Light brown granules were found in cytoplasm of low dose GSPE group (fig. 3C and 4C), yellow granules were found in cytoplasm of medium dose GSPE group (fig. 3D and 4D), and a small number of light yellow granules were found in cytoplasm of high dose GSPE group (fig. 3E and 4E). Table 6 showed the average *A* values of iNOS and calpain Ⅱ protein expression in LECs of each group. Selenite treatment caused a significant increase in the iNOS and calpain Ⅱ protein expression in model group as compared with control group ($P<0.001$) and there were statistically significant differences between adjacent two GSPE-treated groups ($P<0.01$ or $P<0.001$).

Table 6 *A* values of INOS and calpain Ⅱ protein expression in LECs

Groups	iNOS	Calpain Ⅱ
Control	0.051±0.011	0.058±0.006
Model	$0.223\pm0.012^{**}$	$0.200\pm0.010^{**}$
GSPE		
Low dose	$0.170\pm0.009^{**\triangle}$	$0.171\pm0.007^{**\triangle}$
Medium dose	$0.103\pm0.002^{**\triangle\#}$	$0.132\pm0.009^{**\triangle\#}$
High dose	$0.079\pm0.009^{*\triangle\#\bigstar}$	$0.070\pm0.013^{\star\triangle\#\blacktriangle}$

$^{\star}P<0.05$, $^{*}P<0.01$, $^{**}P<0.001$ *vs.* control group; $^{\triangle}P<0.001$ *vs.* model group; $^{\#}P<0.001$ *vs.* low dose GSPE group; $^{\bigstar}P<0.01$, $^{\blacktriangle}P<0.001$ *vs.* medium dose GSPE group

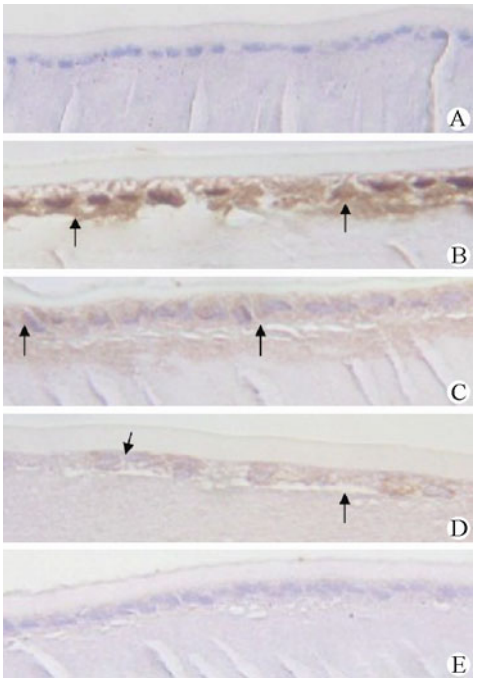

Fig. 3 Immunohistochemical staining of iNOS in LECs (positive cells were directed by arrows, ×400)
A: Control group, negative staining in LECs; B: Model group, a large number of dark brown granules in cytoplasm of LECs; C: Low dose GSPE group, light brown granules in cytoplasm of LECs; D: Medium dose GSPE group, yellow granules in cytoplasm of LECs; E: high dose GSPE group, a small number of light yellow granules in cytoplasm of LECs

2.5 Expression of INOS and Calpain Ⅱ mRNA in Lenses

As shown in table 7 and fig. 5, the iNOS and calpain Ⅱ mRNA expression was detected by using real-time quantitative RT-PCR in rat lenses. Selenite treatment caused a significant increase in the iNOS and calpain Ⅱ mRNA in model group as compared with control group ($P<0.001$). Administration of GSPE led to a dose-dependent reduction in the iNOS and calpain Ⅱ mRNA expression, and there were statistically significant differences between adjacent two GSPE-treated groups ($P<0.05$ or $P<0.01$ or $P<0.001$).

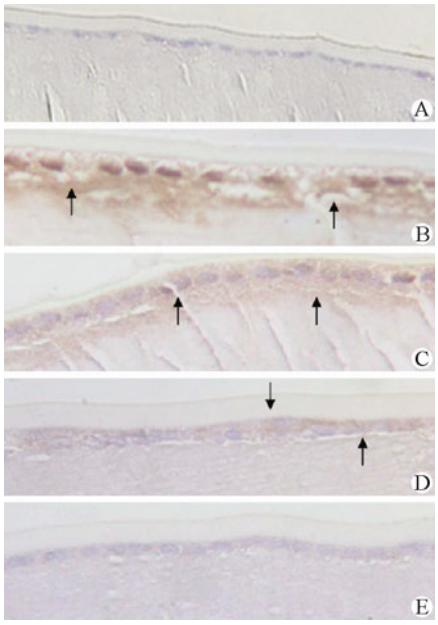

Fig. 4 Immunohistochemical staining of calpainⅡ in LECs (positive cells were directed by arrows, ×400)
A: Control group, negative staining in LECs. B: Model group, a large number of dark brown granules in cytoplasm of LECs; C: Low dose GSPE group, light brown granules in cytoplasm of LECs; D: Medium dose GSPE group, yellow granules in cytoplasm of LECs; E: high dose GSPE group, a small number of weak yellow granules in cytoplasm of LECs

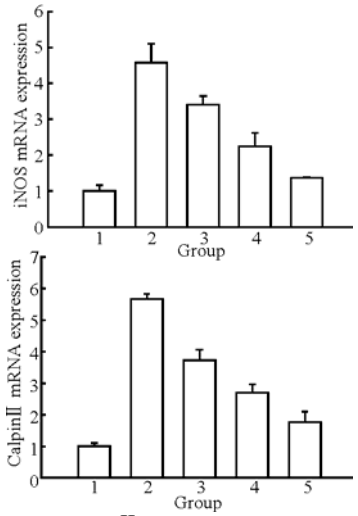

Fig. 5 iNOS and calpainⅡ mRNA expression detected by using real-time quantitative RT-PCR group
1: Control group; 2: Model group; 3: Low dose GSPE group, 4: Medium dose GSPE group; 5 High dose GSPE group

Table 7 INOS and CalpainⅡ mRNA expression in Lenses

Groups	iNOS	CalpainⅡ
Control	1.00±0.16	1.00±0.12
Model	$4.57\pm0.54^{**}$	$5.68\pm0.15^{**}$
GSPE		
Low dose	$3.39\pm0.26^{**\triangle\triangle}$	$3.74\pm0.33^{**\triangle}$
Medium dose	$2.25\pm0.36^{**\triangle\#}$	$2.70\pm0.28^{**\triangle\#}$
High dose	$1.37\pm0.04^{*\triangle\#\bigstar}$	$1.76\pm0.35^{\star\triangle\#\blacktriangle}$

$^{\star}P<0.05$, $^{*}P<0.01$, $^{**}P<0.001$ *vs.* control group; $^{\triangle}P<0.001$ *vs.* model group; $^{\#}P<0.001$ *vs.* low dose GSPE group; $^{\bigstar}P<0.01$, $^{\blacktriangle}P<0.001$ *vs.* medium dose GSPE group

3 DISCUSSION

Cataract is a tough problem worldwide. Yet, a pharmacological treatment against cataract has not been achieved. Although cataract is a multifactorial disease associated with several risk factors, oxidative stress has been suggested as a common underlying mechanism of cataract, and augmentation of the antioxidant defenses of the lens has been shown to prevent or delay experimental cataract[15, 16]. We used selenite-induced cataract as a model to evaluate the preventive efficacy of GSPE.

In our experiment, we found the maximal diameter of nuclear cataract plaques had no statistically significant difference between low lose GSPE group and model group from the postpartum day 15 to 18 ($P>0.05$), and that in other two GSPE-treated groups was significantly reduced ($P<0.05$ or $P<0.001$). Except that there was no statistically significant difference between medium dose and low dose GSPE groups from postpartum day 15 to 16 as well as between medium dose and high dose GSPE groups from postpartum day 15 to 18 ($P>0.05$), there was statistically significant difference between other adjacent two GSPE treated groups ($P<0.05$ or $P<0.01$). We may come to a conclusion that the effect of GSPE is not only dose-dependent but also time-dependent.

SOD, CAT and GSH-PX are important antioxidative enzymes, which make up antioxidative defense system against free radical, eventually protect the cells from oxidative damage. SOD is reported to inhibit hydroxyl radical production, and it reacts with superoxide radicals and converts them to H_2O_2[17]. CAT catalyzes the conversion of H_2O_2 to water and molecular oxygen[18]. GSH-PX catalyzes the reaction of lipid hydroperoxides with glutathione, and converts them to their corresponding alcohols as well as free H_2O_2 to water[19]. MDA is the final production of peroxidation of unsaturated fatty acids, its level is measured as lipid peroxidation index, and it directly reflects the degree of oxidative damage in lenses[20]. In this study, we observed that selenite treatment caused a significant decrease in the activities of SOD, CAT, GSH-PX, accompanied by a significant increase in the levels of MDA in model group as compared with control group ($P<0.01$ or $P<0.001$), suggesting the oxidative damage mechanism in selenite-induced cataract. Treatment with GSPE dose-dependently preserved the activities of these antioxidative enzymes and reduced the generation of MDA as compared with model group ($P<0.05$ or $P<0.01$ or $P<0.001$). There were statistically significant differences between adjacent two GSPE-treated groups ($P<0.05$ or $P<0.01$ or $P<0.001$). Our results suggested that GSPE could protect antioxidative defense system against free radical, augment antioxidant enzyme activities, and reduce generation of lipid peroxidation. Besides, we found there was no statistically significant difference between control group and high dose GSPE group ($P>0.05$). In this experiment, we found the lowest effective dose of GSPE was 50 mg/kg.

Calpains are specific Ca^{2+}-activated neutral proteases found in all tissues. There are several isoforms of calpains in lenses, but the main calpain in rodent and human cataract is calpainⅡ [21]. The increased calcium level may be caused by oxidation of sulfhydryl groups of

proteins in LECs. Oxidative stress-induced lipid peroxidative damage of membranes might be a contributing factor in the loss of Ca^{2+} ATPase activity and accumulation of Ca^{2+}, which in turn leads to the activation of lens calpains and subsequent proteolytic degradation of lens soluble proteins in selenite cataract[22, 23]. In this study, concentration of Ca^{2+} and level of calpain Ⅱ were significantly increased by selenite administration, which confirmed the important roles of Ca^{2+} and calpain Ⅱ in cataract formation (P<0.001). Administration of GSPE was observed to dose-dependently reduce the concentration of Ca^{2+} and level of calpain Ⅱ, suggesting that GSPE suppressed the activation of calpain Ⅱ as well as accumulation of Ca^{2+}, and thus, prevented selenite-induced cataract formation.

INOS is the enzyme that catalyzes the synthesis of NO. It is reported that high levels of iNOS and NO are expressed in lenses of human age-related cataract, which suggests that high level of NO produces oxidative damage to the lenses[24]. INOS is seldom expressed under physiological condition, but when it is activated by induced factors, it generates larger amounts of none physiological concentration of NO than other isoforms of NOS. NO reacts readily with the oxygen free radical and superoxide anion, to form a strong oxidant, peroxynitrite (ONOO-), whose cytotoxic potential is greater than that of NO, and which leads to oxidative damage of protein, nucleic acid and lipid[25]. Though NO and iNOS have been implicated in cataractogenesis, the mechanism remains unclear. In this study, in model group NO and iNOS levels were significantly increased by selenite administration as compared with control group (P<0.001), which confirmed the important roles of NO and iNOS in cataract formation. However, it was found that GSPE treatment dose-dependently reduce the generation of NO and iNOS, which suggested that GSPE suppressed the activation of iNOS, and thus, retarded selenite-induced cataract formation.

In conclusion, intragastric administration of GSPE could retard selenite-induced cataract formation in the *in vivo* model, which provides a new method for pharmacological treatment of cataract in clinical work. The protective effect may be attributed to its excellent antioxidant activity and inhibitory influence on calpain Ⅱ, iNOS activation in lenses. Although the preventive efficacy has been confirmed in this study, further experimental investigation is still required to explore whether GSPE has therapeutic efficacy on already developed cataract.

REFERENCES

1 Thylefors B. Avoidable blindness. Bull World Health Organ, 1999,77(6):453
2 Thylefors B. Global data on blindness. Bull World Health Organ, 1995,73(1):115-121
3 Olson RJ, Mamalis N, Werner L, *et al*. Cataract treatment in the beginning of the 21st century. Am J Ophthalmol, 2003,136(1):146-154
4 Truscott RJ. Age related nuclear cataract—oxidation is the key. Exp Eye Res, 2005,80(2):709-725
5 Sakthivel M, Elanchezhian R, Ramesh E, *et al*. Prevention of selenite-induced cataractogenesis in Wistar rats by the polyphenol, ellagic acid. Exp Eye Res, 2008,86(2): 251-259
6 Thomas R, Hong Ma, Chiho Fukiage, *et al*. Selenite nuclear cataract: review of the model. Mol Vis, 1997,3:8
7 Bagchi D, Garg A, Krohn RL, *et al*. Protective effects of grape seedproanthocyanidins and selected antioxidants against TPA-induced hepatic and brain lipid peroxidation and DNA fragmentation, and peritoneal macrophage activation in mice. Gen Pharmacol, 1998,30(5):771-776
8 Bagchi D, Garg A, Krohn RL, *et al*. Oxygen free radical scavenging abilities of vitamins C and E, and a grape seed proanthocyanidin extract *in vitro*. Res Commun Mol Pathol Pharmacol, 1997,95(2):179-189
9 Debasis B, Manashi B, Sidney JS, *et al*. Free radicals and grape seed proanthocyanidin extract: importance in human health and disease prevention. Toxicology, 2000,148(2-3):187-197
10 Ito Y, Nabekura T, Takeda M, *et al*. Nitric oxide participates in cataract development in selenite-treated rats. Curr Eye Res, 2001,22(3):215-220
11 Biju PG, Rooban BN, Lija Y, *et al*. Drevogenin D prevents selenite-induced oxidative stress and calpain activation in cultured rat lens. Mol Vis, 2007, 13:1121-9
12 Manikandan R, Thiagarajan R, Beulaja S, *et al*. Anti-cataractogenic effect of curcumin and aminoguanidine against selenium-induced oxidative stress in the eye lens of Wistar rat pups: An *in vitro* study using isolated lens. Chem Biol Interact, 2009,181(2):202-209
13 Hiraoka T, Clark JI. Inhibition of lens opacification during the earlystages of cataract formation. Invest Ophthalmol Vis Sci, 1995,36(12):2550-2555
14 Livak KJ, Schmittgen TD. Analysis of relative gene expression data using real-time quantitative PCR and the 2(-Delta Delta C(T)) method. Methods, 2001,25(4): 402-408
15 Spector A. Oxidative stress induced cataract: mechanism of action. FASEB J, 1995,9(12):1173-1182
16 Henein M, Morris S, Varma SD, *et al*. Prevention of selenite cataract by vitamin C. Exp Eye Res, 1991,52(5): 563-568
17 Behndig A, Svensson B, Marklund SL, *et al*. Superoxide dismutase isoenzymes in the human eye. Invest Ophthalmol Vis Sci, 1998,39(3):471-475
18 Yang Y, Spector A, Ma W, *et al*. The effect of catalase amplification on immortal lens epithelial cell lines. Exp Eye Res, 1998,67(6):647-656
19 Manikandan R, Thiagarajan R, Beulaja S, *et al*. Effect of curcumin on selenite induced cataractogenesis in Wistar rat pups. Curr Eye Res, 2010,35(2):122-129
20 Wang D, Li Y, Hou G, *et al*. Pygeum africanum: effect on oxidative stress in early diabetes-induced bladder. Int Urol Nephrol, 2009,42(2):401-408
21 Biswas S, Harris F, Singh J, *et al*. Role of calpains in diabetes mellitus-induced cataractogenesis: a mini review, Mol Cell Biochem, 2004,261(1-2):15l-159
22 Ahuja RP, Borchman D, Dean WL, *et al*. Effect of oxidation on Ca^{2+}-ATPase activity and membrane lipids in lens epithelial microsomes. Free Radic Biol Med, 1999,27 (1-2):177-185
23 Wang Z, Bunce GE, Hess JL. Selenite and Ca^{2+} homeostasis in the rat lens: effect on Ca^{2+}-ATPase and passive Ca^{2+} transport. Curr Eye Res, 1993,12(3):213-218
24 Kemal O, Fatih K, Zeliha B. May nitric oxide molecule have a role in the pathogenesis of human cataract? Exp Eye Res, 2003,76(1):23-27
25 Beckman JS, Beckman TW, Chen J, *et al*. Apparent hydroxyl radical production by peroxynitrite: Implication for endothelial injury from nitric oxide and superoxide. Proc Natl Acad Sci USA, 1990,87(4):1620-1624

(Received Oct. 24, 2011)